Original Article

Radiomics based on machine learning algorithms could predict prognosis and postoperative chemotherapy benefits of patients with gastric cancer: a retrospective cohort study

Yilan Xiang[1#], Yuanbo Hu[2#], Chenbin Chen[2#], Huaiqing Zhi[2], Zhao Zhang[1], Mingdong Lu[3], Xietao Chen[2], Zhixian Luo[1], Sian Chen[4], Emmanuel Dias-Neto[5,6], Paolo Pizzini[7], Xinxin Chen[3], Xiaodong Chen[2*], Yuandi Zhuang[1*], Qiantong Dong[2*]

[1]Department of Radiology, The First Affiliated Hospital of Wenzhou Medical University, Wenzhou, China; [2]Department of General Surgery, The First Affiliated Hospital of Wenzhou Medical University, Wenzhou, China; [3]Department of General Surgery, The Second Affiliated Hospital & Yuying Children's Hospital of Wenzhou Medical University, Wenzhou, China; [4]Department of Emergency, The Second Affiliated Hospital & Yuying Children's Hospital of Wenzhou Medical University, Wenzhou, China; [5]Laboratory of Medical Genomics, A. C. Camargo Cancer Center, São Paulo, SP, Brazil; [6]Division of Cancer Biology, Department of Radiation Oncology, Rutgers New Jersey Medical School, Newark, NJ, USA; [7]Department of Digestive Surgery, European Institute of Oncology-IRCCS, Milan, Italy

Contributions: (I) Conception and design: Y Xiang, Xiaodong Chen, Y Zhuang, Q Dong; (II) Administrative support: Xiaodong Chen, M Lu, Q Dong; (III) Provision of study materials or patients: Y Xiang, Y Hu, C Chen, M Lu, Xietao Chen, Q Dong; (IV) Collection and assembly of data: Y Xiang, Y Hu, C Chen, H Zhi, Z Zhang, Xietao Chen, Z Luo, S Chen, Xinxin Chen; (V) Data analysis and interpretation: Y Xiang, Y Hu, C Chen, H Zhi; (VI) Manuscript writing: All authors; (VII) Final approval of manuscript: All authors.

[#]These authors contributed equally to this work as co-first authors.

[*]These authors contributed equally to this work as co-corresponding authors.

Correspondence to: Qiantong Dong, PhD. Department of General Surgery, The First Affiliated Hospital of Wenzhou Medical University, Nanbaixiang, Ouhai District, Wenzhou 325015, China. Email: dongqt2021@wmu.edu.cn; Yuandi Zhuang, MD. Department of Radiology, The First Affiliated Hospital of Wenzhou Medical University, Nanbaixiang, Ouhai District, Wenzhou 325015, China. Email: viaviahei@163.com; Xiaodong Chen, MD. Department of General Surgery, The First Affiliated Hospital of Wenzhou Medical University, Nanbaixiang, Ouhai District, Wenzhou 325015, China. Email: 15167797063@163.com.

Background: Traditional clinical characteristics have certain limitations in evaluating cancer prognosis. The radiomics features provide information on tumor morphology, tissue texture, and hemodynamics, which can accurately reflect personalized predictions. This study investigated the clinical value of radiomics features on contrast-enhanced computed tomography (CT) images in predicting prognosis and postoperative chemotherapy benefits for patients with gastric cancer (GC).

Methods: For this study, 171 GC patients who underwent radical gastrectomy and pathology confirmation of the malignancy at the First Affiliated Hospital of Wenzhou Medical University were retrospectively enrolled. The general information, pathological characteristics, and postoperative chemotherapy information were collected. Patients were also monitored through telephone interviews or outpatient treatment. GC patients were randomly divided into the developing cohort (n=120) and validation cohort (n=51). The intra-tumor areas of interest inside the tumors were delineated, and 1,218 radiomics features were extracted. The optimal radiomics risk score (RRS) was constructed using 8 machine learning algorithms and 29 algorithm combinations. Furthermore, a radiomics nomogram that included clinicopathological characteristics was constructed and validated through univariate and multivariate Cox analyses.

Results: Eleven prognosis-related features were selected, and an RRS was constructed. Kaplan-Meier curve analysis showed that the RRS had a high prognostic ability in the developing and validation cohorts (log-rank P<0.01). The RRS was higher in patients with a larger tumor size (≥3 cm), higher Charlson score (≥2), and higher clinical stage (Stages III and IV) (all P<0.001). Furthermore, GC patients with a higher RRS significantly benefited from postoperative chemotherapy. The results of univariate and multivariate Cox regression analyses demonstrated that the RRS was an independent risk factor for overall survival (OS) and

disease-free survival (DFS) (P<0.001). A visual nomogram was established based on the significant factors in multivariate Cox analysis (P<0.05). The C-index was 0.835 (0.793–0.877) for OS and 0.733 (0.677–0.789) for DFS in the developing cohort. The calibration curve also showed that the nomogram had good agreement.

Conclusions: A nomogram that combines the RRS and clinicopathological characteristics could serve as a novel noninvasive preoperative prediction model with the potential to accurately predict the prognosis and chemotherapy benefits of GC patients.

Keywords: Gastric cancer (GC); computed tomography (CT); radiomics risk score (RRS); machine learning algorithms; postoperative chemotherapy

Submitted Jul 27, 2023. Accepted for publication Oct 20, 2023. Published online Oct 27, 2023.
doi: 10.21037/jgo-23-627
View this article at: https://dx.doi.org/10.21037/jgo-23-627

Introduction

Gastric cancer (GC) is the fifth most common malignant tumor in the world and the third leading cause of cancer-related deaths (1). China has one of the highest incidence rates of GC in the world. It has been reported that annually, approximately 50% of new GC cases occur in China, which seriously threatens public health and increases the economic burden (2). In recent years, the 5-year overall survival (OS) rate of patients with advanced GC was less than 10% (3), although great progress has been made in comprehensive treatment based on surgery. Therefore, precise and personalized prognosis prediction could better assist physicians in comprehending the risks associated with disease progression and provide them with a solid scientific foundation for devising optimal treatment strategies. TNM-based staging reflects the overall characteristics of the tumor at the macro level and is the most commonly used model for GC prognosis evaluation (4). However, this approach is certainly not comprehensive to encompass all elements involving prognosis and cancer-associated mortality. In this sense, individual differences of GC patients, including tumor stage at diagnosis, general health aspects, microbiota and immune-regulation, and tumor microenvironment composition, act in combination to determine prognosis. A focus in tumor tissue analysis has made clear that the development of new methods to deeply evaluate the tissue characteristics of GC (5-7) may be capable of accurately predicting the clinical outcome of GC patients.

Radiomics has been introduced as an emerging technology that extracts high-dimensional radiomic features from standard-of-care medical images and then selects critical features as a signature for quantitative disease diagnostics (8,9). Compared to conventional imaging features from computed tomography (CT), radiomics is considered to have the potential ability to reveal disease characteristics that would go unnoticed by the naked eye. Therefore, models constructed based on radiomics features could make personalized predictions based on the unique features and tumor manifestations of each patient. This helps to determine the survival risk of patients and provides a basis for developing personalized treatment plans more accurately. Several studies have shown that radiology has a good predictive ability in subtype classification (10,11), staging evaluation (12), clinical outcome (13-16), and

Highlight box

Key findings

- A radiomics risk score (RRS) based on enhanced computed tomography (CT) images is a valuable tool for prognostic prediction in gastric cancer (GC) patients.
- RRS could help assess the benefit of postoperative chemotherapy in GC patients.

What is known and what is new?

- TNM stage is widely recognized as the primary determinant impacting the prognosis and treatment decisions for GC patients. Enhanced CT has important application value in early detection, staging diagnosis, and treatment monitoring.
- Radiomics comprehensively analyzes tumor area's multidimensional features, providing objective and reliable results for predicting the prognosis of GC patients. A visual nomogram could further offer personalized prognosis predictions for GC patients.

What is the implication, and what should change now?

- Personalized nomograms based on radiomics and clinicopathologic features are crucial for evaluating the prognosis.
- With the application of radiomics analysis, personalized prediction of postoperative chemotherapy benefits and survival status could guide clinical treatment.

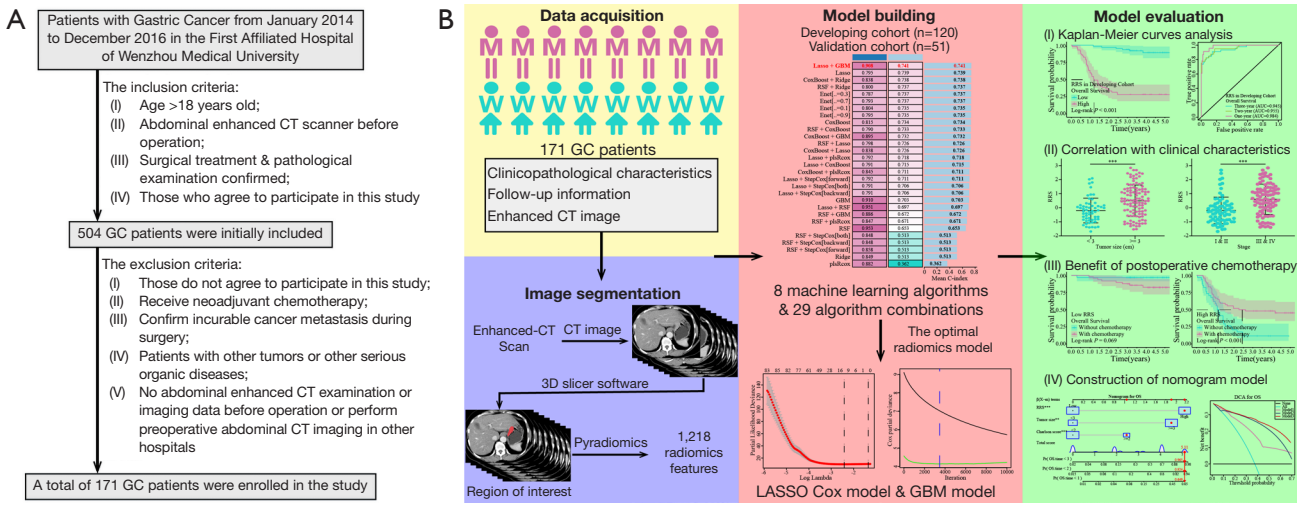

Figure 1 Flow chart of RRS construction and validation. (A) Flow chart for screening patients with GC in this study. (B) The pattern diagram displays the construction and validation of the RRS and clinical prediction model. **, P<0.01; ***, P<0.001. RRS, radiomics risk score; CT, computed tomography; GC, gastric cancer; LASSO, least absolute shrinkage and selection operator; GBM, generalized boosted regression model; RSF, random survival forest; Enet, elastic network; plsRcox, partial least squares regression for Cox; OS, overall survival; DCA, decision curve analysis.

treatment response of tumor patients (17,18). Moreover, machine learning has unique advantages in processing high-dimensional data and finding feature variables (19-21). However, to the best of our knowledge, there have been few reports on the prediction of survival prognosis and chemotherapy response in GC patients using radiomics analysis along with multiple machine learning algorithm combinations.

In this study, we attempted to use 8 machine learning algorithms and 29 algorithm combinations to establish and validate an optimal risk score model for 1,218 radiomics features in developing and validation cohorts to evaluate the prognosis, recurrence, and chemotherapy benefits of GC patients. We built a nomogram model based on the risk model and clinicopathological characteristics to help evaluate precise treatment and further improve the clinical outcome of GC patients. We present this article in accordance with the CLEAR and TRIPOD reporting checklists (available at https://jgo.amegroups.com/article/view/10.21037/jgo-23-627/rc).

Methods

Patients

GC patients who underwent radical surgery in the First Affiliated Hospital of Wenzhou Medical University from January 2014 to December 2016 were included retrospectively. None of the patients received chemotherapy or radiotherapy before surgery, and all patients were diagnosed with gastric adenocarcinoma by histopathology. All operations were performed by experienced surgeons. Furthermore, the perioperative treatment and management of GC patients were based on the Japanese GC Treatment Guidelines 2010 (version 3) (22) and the Guidelines for GC Diagnosis and Treatment from the Chinese Anti-Cancer Association (23). The inclusion criteria were: (I) age >18 years old; (II) abdominal enhanced CT scan before operation; (III) gastric adenocarcinoma confirmed by surgical treatment and pathological examination; and (IV) agreement to participate in this study. The exclusion criteria were as follows: (I) patients who did not agree to participate in this study; (II) patients who received neoadjuvant chemotherapy; (III) patients with confirmed incurable cancer metastasis during surgery; (IV) patients with other tumors or other serious organic diseases; and (V) patients with no abdominal enhanced CT examination or imaging data before the operation or who underwent preoperative abdominal CT imaging in other hospitals. The flow chart for patient screening is shown in *Figure 1A*. The study was conducted in accordance with the Declaration of Helsinki (as revised in 2013). The Ethics Committee of The First Affiliated Hospital of Wenzhou Medical University

approved this research (No. KY2021-R092). Considering this was a retrospective study that did not impose additional costs or harm on patients, informed consent from the patients was not required.

Data collection and follow-up

The clinicopathological data of all patients enrolled in the study were collected retrospectively. General information included the patient's disease characteristics before surgery, such as age, sex, body mass index (BMI), Nutritional Risk Screening 2002 (NRS 2002) scores, hemoglobin, and Charlson score. Other characteristics included pathological characteristics of the tumor, postoperative chemotherapy regimen, chemotherapy cycle, and time to relapse and death. Patients with complete clinical data were selected for subsequent analysis. The patient's postoperative adjuvant chemotherapy regimen and cycle followed the National Comprehensive Cancer Network (NCCN) (2013 and 2016 versions) guidelines (24,25). In this study, patients undergoing postoperative chemotherapy received either oxaliplatin and capecitabine (XELOX) regimen or tegafur-gimeracil-oteracil potassium capsules (S-1) and oxaliplatin (SOX) regimen treatment. Patients who completed at least three cycles of adjuvant chemotherapy after surgery were confirmed to have received chemotherapy; otherwise, they were considered to have not received postoperative chemotherapy.

The routine outpatient examination was performed for each patient after the operation. Patients were monitored every 3 months during the first 2 years and then every 6 months through telephone interview or outpatient treatment. The outcome analysis was double-blind throughout the follow-up. At every follow-up visit, we obtained a medical history and performed a physical examination, which included blood biochemistry, blood tumor markers, abdominal CT scanning and gastroscopy. During follow-up, we defined OS as the time interval from the date of surgery to the date of death for any reason. Disease-free survival (DFS) was calculated from the date of surgery to the date of first recurrence in any area or death due to any reason, whichever occurred first. Patients were followed up starting from the time of gastrectomy and censored at the last alive contact or at the end point of data collection for this study (29 February 2020).

CT image acquisition parameters

The study adhered to the CLEAR checklist for conducting and reporting experimental research (26). All patients were scanned with a 64-slice spiral CT scanner (VCT, GE Healthcare, Chicago, IL, USA) or an Aquilion ONE 320 slice CT scanner (Canon, Tokyo, Japan) within one month before surgery as the baseline abdominal CT. The scanning range was from the tip of the diaphragm to the lower edge of the pubic symphysis, covering the upper abdomen or the whole abdomen. For contrast-enhanced CT, nonionic contrast agent (iopromide: 370 mg I/mL) and saline were injected with an automatic syringe, and the injection dose depended on the patient's weight. The scanning process was intelligently triggered by monitoring the abdominal aorta, in which the arterial phase was delayed by 30–35 s, and the portal phase was delayed by 60–70 s. If necessary, a delayed scan was performed with a 180 s delay. During scanning, the relevant parameters of image acquisition were as follows: tube voltage, 120 kV; tube current, 150–190 mAs; rotation time, 0.5 s; detector collimation, 8 mm × 2.5 mm or 64 mm × 0.625 mm; field of view, 350 mm × 350 mm; and matrix, 512×512. The reconstruction thickness of contrast-enhanced CT was 5 mm. Next, portal venous phase CT images were obtained from the Picture Archiving and Communication System (PACS) (Carestream, Rochester, NY, USA) for subsequent standardized processing and analysis (27).

Image segmentation and radiomics feature extraction

3D Slicer software (version 4.10.2; http://www.slicer.org) was used for selection of the region of interest (ROI) and image segmentation. First, an experienced radiologist (Y.X.) and a general surgeon (Y.H.) drew the tumor focus randomly and independently without assessing any clinicopathological characteristics or outcomes of these patients. Then, a senior radiologist (Z.Z.) re-evaluated and ensured the accuracy of segmentation until consensus was reached. After that, the radiologist (Y.X.) randomly selected 50 patients and segmented their ROI again one month later to evaluate the consistency of ROI image quality.

Next, radiomics features were extracted from the tumor image ROI using the Pyradiomics package (28) (version 3.7.2), an open-source Python package. The feature extraction parameters were adjusted as follows: resample PixelSpacing: [1, 1, 1], padDistance: 10, binWidth: 25, Original: (), Wavelet: (), LoG: sigma: [1.0, 2.0, 3.0, 4.0, 5.0]. The remaining parameters were set to the default values. The radiomics features were as follows: (I) first-

order statistics; (II) shape-based features; (III) gray-level cooccurrence matrix (GLCM); (IV) gray-level run length matrix (GLRLM); (V) gray-level size zone matrix (GLSZM); and (VI) gray-level dependence matrix (GLDM). We applied wavelet filters and Laplace Gaussian filters with different sigma values to the original CT images to obtain higher-order statistical features. In total, 1,218 radiomics features were extracted from the original and filtered images.

Dimension reduction and development of the radiomics risk score (RRS)

To screen the prognostic imaging characteristics of GC, we randomly divided all patients into developing and validation cohorts at a ratio of 7:3. The intraclass correlation coefficients (ICCs) of 1,218 radiomics features from 50 patients pre- and post-segmentation were calculated to evaluate the repeatability of the data. Highly consistent features were considered to be those with ICC values >0.75 were defined as high consistency features. Furthermore, the high consistency features of all patients were standardized by the z score algorithm using the mean and standard deviation (SD) of the developing cohort (29).

Next, we integrated 8 machine learning algorithms and 29 algorithm combinations to build the optimal radiomics model for predicting the prognosis of GC patients (30). The machine learning algorithms included random survival forest (RSF), elastic network (Enet), least absolute shrinkage and selection operator (LASSO), ridge, stepwise Cox, CoxBoost, partial least squares regression for Cox (plsRcox), and generalized boosted regression model (GBM). In the developing cohort, 29 algorithm combinations were calculated for the high consistency features of patients, and the corresponding prediction model was constructed through cross validation. All models were further validated in GC patients from the validation cohort. Furthermore, the Harrell consistency index (C-index) of each prediction model in the developing and validation cohorts was calculated. The model with the highest C-index in the validation group was considered to be the best model for the subsequent analysis. According to the optimal prediction model, the corresponding risk score of each patient in the developing and validation cohorts was calculated and defined as the RRS. According to the best cutoff value of the RRS of GC patients in the developing cohort (RRS =0.10), we divided all patients into high-risk and low-risk groups.

Construction and validation of the clinical nomogram prediction model

After establishment of the RRS, the clinicopathological characteristics and RRS of GC patients in the developing cohort were selected for further univariate and multivariate Cox analyses to obtain prognosis-related clinical characteristics. Then, we selected clinical features with $P<0.05$ and constructed a nomogram to visualize the results for application in clinical practice. The C-index of the nomogram was calculated to evaluate the differentiation performance of the model. The predicted values of the nomogram were compared with the observed actual survival rate, and a calibration curve was drawn to recalibrate the performance of the nomogram in the validation cohort. Furthermore, decision curve analysis (DCA) was performed to evaluate the stability and reliability of the risk prediction model.

Statistical analysis

All statistical analyses were performed using R (https://www.r-project.org/, version 4.1.3). Continuous variables were compared using an unpaired Student's t test, whereas categorical variables were compared using the chi-square test or Fisher's exact test. Univariate and multivariate Cox regressions were analyzed to obtain the independent risk factors for prognosis. The Kaplan-Meier method was used to generate survival curves, and the log-rank test was used to compare the differences between two groups. The timeROC package (version 0.40) was utilized for plotting receiver operating characteristic (ROC) curves and calculating AUC values to assess the accuracy of RRS predictions for prognosis. Furthermore, the radiomics quality score (RQS) developed by Lambin *et al.* serves as a scoring system to evaluate the quality and reliability of radiomics studies (31). The RQS was calculated to evaluate the quality of this study.

Results

Clinical characteristics of the patients

According to the inclusion and exclusion criteria, 504 GC patients who underwent radical surgery and preoperative enhanced CT examination were initially included. However, the images of 333 (66.1%) GC patients could not undergo further image segmentation and were excluded from this study due to poor image quality, caused by poor gastric filling, metal artifacts, or large amounts of food residue in the stomach. Finally, a total of 171 GC

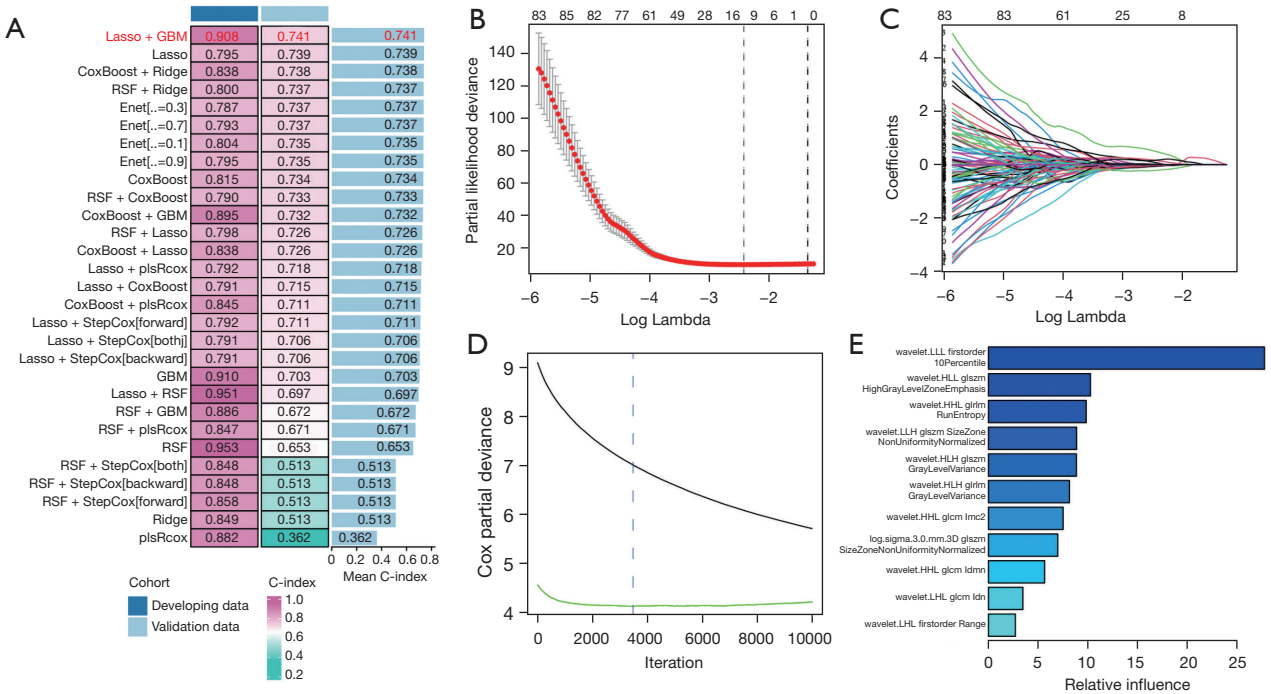

Figure 2 RRS was constructed and validated based on different machine learning combinations. (A) Based on the radiomics features, 8 machine learning algorithms and 29 algorithm combinations were used to construct GC patient prediction models, and the corresponding C-index of different models in the developing and validation cohorts was calculated. The C-index values of 29 models in the validation group were sorted and visualized. (B) Partial likelihood deviation values corresponding to the λ values of LASSO models. The dotted line represents the optimal λ value and the simplest λ value. (C) The optimal λ value was selected, and the LASSO coefficient corresponding to the important imaging characteristics was obtained. (D) The relationship between the number of different learners in the GBM and the Cox partial deviance to prevent overfitting of the model. The blue line represents the best number of learners using cross validation. (E) The relative influence of different radiomics features in the GBM. RRS, radiomics risk score; GC, gastric cancer; LASSO, least absolute shrinkage and selection operator; GBM, generalized boosted regression model; RSF, random survival forest; Enet, elastic network; plsRcox, partial least squares regression for Cox.

patients were enrolled in the study. The average age of the enrolled patients was 65.23±10.69 years old, and most were males (N=131, 76.6%). The average follow-up time was 35.94±19.83 months, and 68 patients (39.8%) died during the study period. The flow chart of patient selection is shown in *Figure 1A*.

Next, the 171 GC patients were randomly divided into a developing cohort (n=120) and a validation cohort (n=51). We compared the clinicopathological characteristics of the developing and validation cohorts using the chi-square test. The results showed that only the Charlson score was significantly different between the two cohorts (P=0.022). There were no significant differences in the other clinicopathological characteristics (P>0.050). The clinicopathological characteristics of the patients in the developing and validation cohorts are listed in Table S1.

Construction of the RRS as a novel prognostic marker

To better reflect the influence of tumor tissue characteristics on the prognosis of GC patients, we segmented tumor tissue images and extracted 1,218 radiomics features at different levels. The results showed that the average ICCs of all features was 0.91±0.17. Using the criterion of an ICC value greater than 0.75, we selected 1,077 features with high consistency for subsequent model construction. The workflow of the RRS prognostic model construction is shown in *Figure 1B*. In the developing cohort, we used 29 algorithm combinations and cross validation to reduce the dimension and screen the prognosis-related radiomics features and then fitted the corresponding prediction model. Furthermore, we calculated the C-index of each model in the developing and validation cohorts (*Figure 2A*). Interestingly, the combined

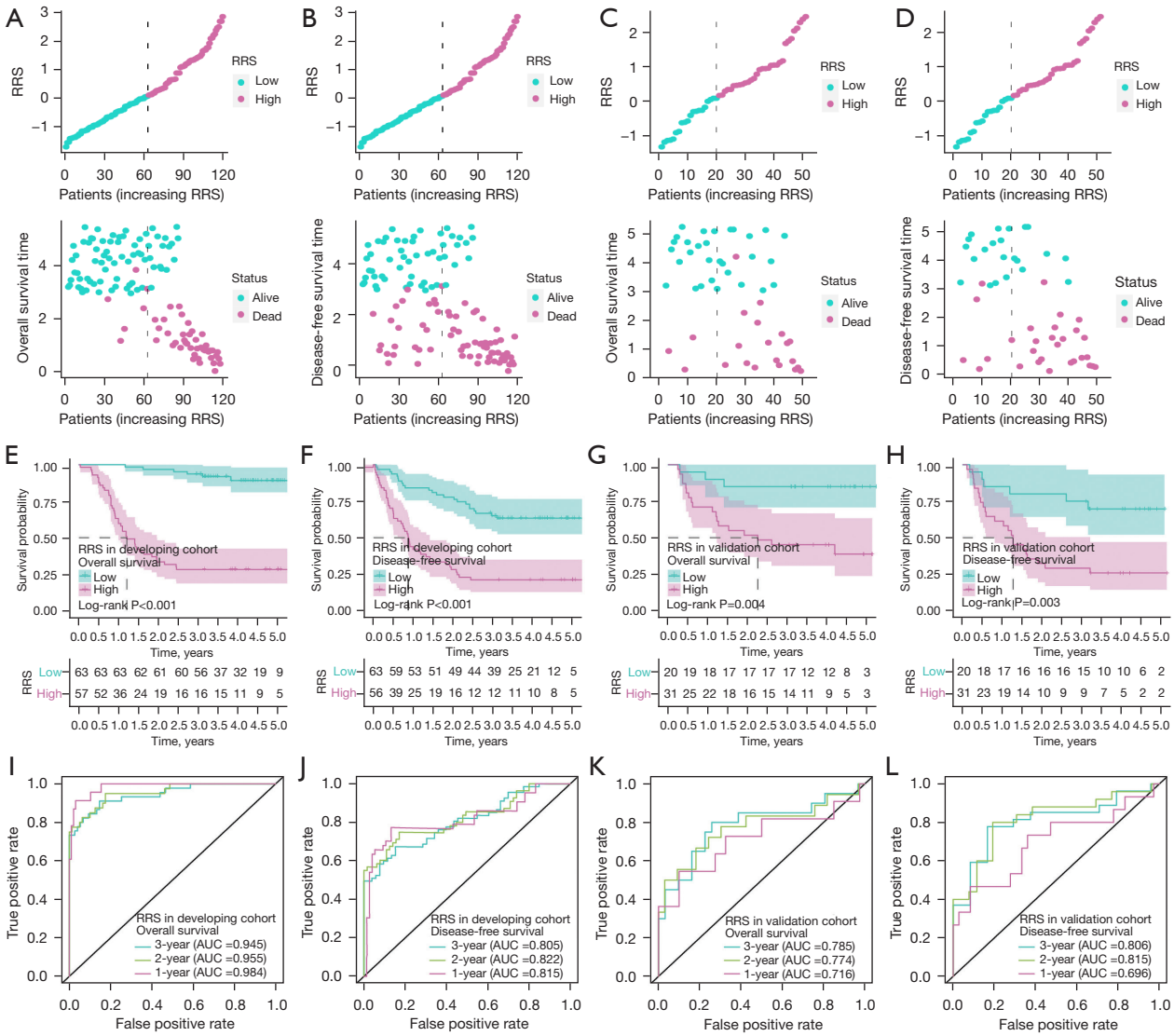

Figure 3 RRS was a better prognostic marker for GC patients. (A,B) The distribution characteristics between RRS, survival status and survival time of GC patients in the developing cohort. (C,D) The distribution characteristics between RRS, survival status and survival time of GC patients in the validation cohort. (E,F) Kaplan-Meier curve analysis of OS and DFS between the high and low RRS groups in the developing cohort. (G,H) Kaplan-Meier curve analysis of OS and DFS between the high and low RRS groups in the validation cohort. (I,J) Time-dependent ROC curve analysis of RRS for OS and DFS in the developing cohort. (K,L) Time-dependent ROC curve analysis of the RRS in the validation cohort. RRS, radiomics risk score; GC, gastric cancer; OS, overall survival; DFS, disease-free survival; ROC, receiver operating characteristic; AUC, area under curve.

algorithm of LASSO and GBM had the highest C-index in the validation cohort (0.741). Using LASSO Cox analysis, we obtained the best value and 11 prognosis-related features with a nonzero LASSO coefficient through the minimum value of partial likelihood deviation (*Figure 2B*,*2C*). Next, the GBM was performed, and the best number of iterations was used to further construct the prognostic model for the 11 features (*Figure 2D*). The relative importance of each feature is shown in *Figure 2E*.

Then, we calculated the risk score for each patient, termed the RRS. All GC patients were divided into high-risk and low-risk groups according to the best cutoff value of the RRS (RRS =0.10). *Figure 3A-3D* displays the correlation and distribution of RRS, survival status

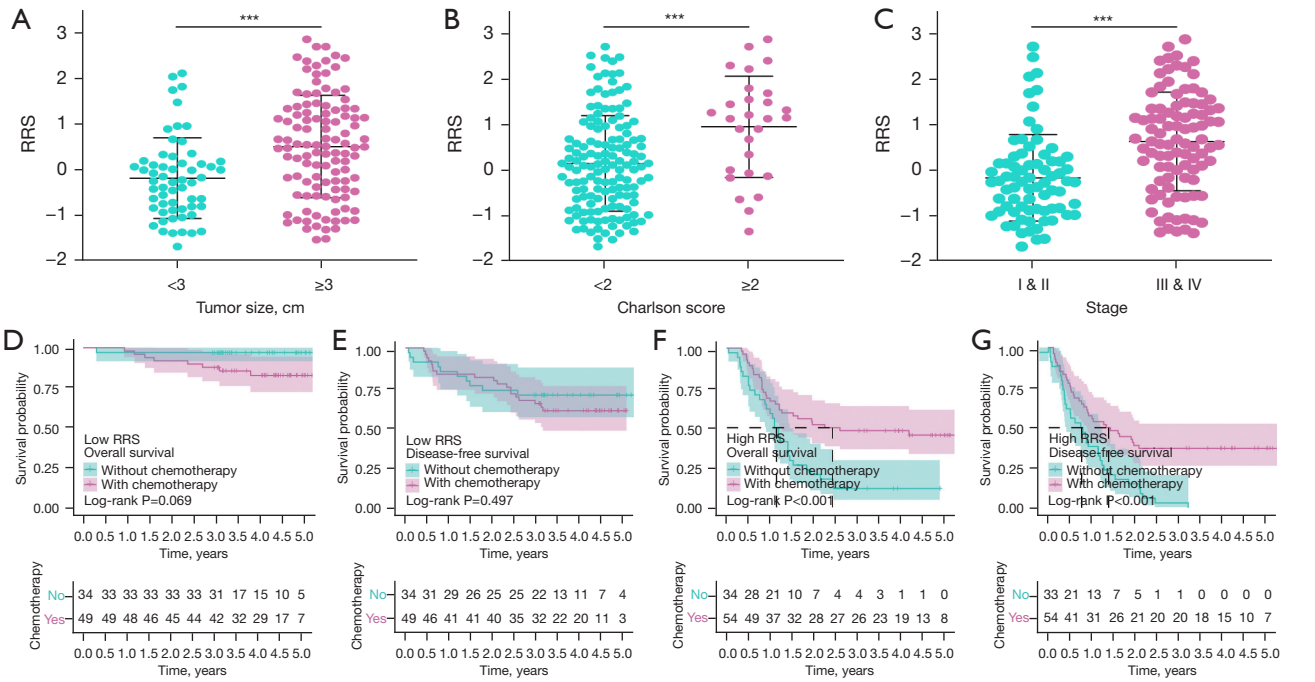

Figure 4 Correlation analysis between RRS and different clinicopathological characteristics. (A) The difference in RRS between different tumor sizes in GC patients. (B) The difference in RRS between different Charlson scores in GC patients. (C) The difference in RRS between different clinical stages in GC patients. (D) Kaplan-Meier curve analysis of OS between GC patients with low RRS who received and did not receive postoperative chemotherapy. (E) Kaplan-Meier curve analysis of DFS between GC patients with low RRS who received and did not receive postoperative chemotherapy. (F) Kaplan-Meier curve analysis of OS between GC patients with a high RRS who received and did not receive postoperative chemotherapy. (G) Kaplan-Meier curve analysis of DFS between GC patients with a high RRS who received and did not receive postoperative chemotherapy. ***, P<0.001. RRS, radiomics risk score; GC, gastric cancer; OS, overall survival; DFS, disease-free survival.

and survival time of each patient in the developing and validation cohorts, including OS and DFS. In the developing cohort, the survival analysis results showed that compared with GC patients with a low RRS, those with a high RRS had a poor clinical prognosis (OS: log-rank P<0.001, *Figure 3E*; DFS: log-rank P<0.001, *Figure 3F*). The survival analysis in the validation group also showed that GC patients with a high RRS had a relatively poor prognosis (OS: log-rank P=0.004, *Figure 3G*; DFS: log-rank P=0.003, *Figure 3H*). Furthermore, the time-dependent receiver operating characteristic (ROC) curve further proved that the RRS had good predictive ability for the OS and DFS of GC patients at 1, 2, and 3 years in the development and validation cohorts (development cohort: *Figure 3I,3J*; validation cohort: *Figure 3K,3L*). Therefore, the RRS model was a better prediction model for the prognosis of GC patients.

RRS was associated with different clinicopathological characteristics and postoperative chemotherapy benefit

Next, we further analyzed the correlation between the RRS and different clinicopathological characteristics. The difference analysis results showed that the RRS was significantly higher in patients with larger tumor tissue sizes (≥3 cm) (P<0.001, *Figure 4A*) and higher Charlson score (≥2) (P<0.001, *Figure 4B*). Furthermore, compared with GC patients with early clinical stage (Stages I and II), the RRS of patients with advanced clinical stage (Stages III and IV) was significantly higher (P<0.001, *Figure 4C*). The distribution of clinicopathological features in GC patients with high and low RRS is shown in *Table 1*.

In addition, we further analyzed the influence of the RRS model on the proportion of GC patients that benefited from postoperative chemotherapy. Of all GC patients involved in the study, 103 patients (59.88%) received complete

Table 1 Comparison of clinicopathological characteristics between GC patients with low and high RRS in the developing and validation cohorts

Variables	Developing cohort				Validation cohort			
	All patients (n=120)	Low RRS (n=63)	High RRS (n=57)	P value	All patients (n=51)	Low RRS (n=20)	High RRS (n=31)	P value
Age (years)				0.052				0.668
≤70	81 (67.5)	48 (76.2)	33 (57.9)		30 (58.8)	13 (65.0)	17 (54.8)	
>70	39 (32.5)	15 (23.8)	24 (42.1)		21 (41.2)	7 (35.0)	14 (45.2)	
Gender				0.768				>0.99
Female	27 (22.5)	13 (20.6)	14 (24.6)		13 (25.5)	5 (25.0)	8 (25.8)	
Male	93 (77.5)	50 (79.4)	43 (75.4)		38 (74.5)	15 (75.0)	23 (74.2)	
BMI (kg/m^2)				0.349				0.547
Low	7 (5.8)	2 (3.2)	5 (8.8)		2 (3.9)	0 (0.0)	2 (6.5)	
Normal	86 (71.7)	45 (71.4)	41 (71.9)		39 (76.5)	15 (75.0)	24 (77.4)	
High	27 (22.5)	16 (25.4)	11 (19.3)		10 (19.6)	5 (25.0)	5 (16.1)	
Anemia				0.941				0.394
No	68 (56.7)	35 (55.6)	33 (57.9)		23 (45.1)	11 (55.0)	12 (38.7)	
Yes	52 (43.3)	28 (44.4)	24 (42.1)		28 (54.9)	9 (45.0)	19 (61.3)	
Charlson score				0.011*				>0.99
<2	95 (79.2)	56 (88.9)	39 (68.4)		48 (94.1)	19 (95.0)	29 (93.5)	
≥2	25 (20.8)	7 (11.1)	18 (31.6)		3 (5.9)	1 (5.0)	2 (6.5)	
Location				0.148				0.179
Cardia	20 (16.7)	13 (20.6)	7 (12.3)		13 (25.5)	3 (15.0)	10 (32.3)	
Body	29 (24.2)	18 (28.6)	11 (19.3)		9 (17.6)	6 (30.0)	3 (9.7)	
Pylorus	63 (52.5)	30 (47.6)	33 (57.9)		28 (54.9)	11 (55.0)	17 (54.8)	
All	8 (6.7)	2 (3.2)	6 (10.5)		1 (2.0)	0 (0.0)	1 (3.2)	
Tumor size (cm)				P<0.001***				0.449
<3	43 (35.8)	34 (54.0)	9 (15.8)		16 (31.4)	8 (40.0)	8 (25.8)	
≥3	77 (64.2)	29 (46.0)	48 (84.2)		35 (68.6)	12 (60.0)	23 (74.2)	
Nerve invasion				0.338				>0.99
No	84 (70.0)	47 (74.6)	37 (64.9)		38 (74.5)	15 (75.0)	23 (74.2)	
Yes	36 (30.0)	16 (25.4)	20 (35.1)		13 (25.5)	5 (25.0)	8 (25.8)	
Vascular invasion				0.459				>0.99
No	89 (74.2)	49 (77.8)	40 (70.2)		41 (80.4)	16 (80.0)	25 (80.6)	
Yes	31 (25.8)	14 (22.2)	17 (29.8)		10 (19.6)	4 (20.0)	6 (19.4)	
Stage				P<0.001***				0.445
Stage I	18 (15.0)	12 (19.0)	6 (10.5)		7 (13.7)	4 (20.0)	3 (9.7)	
Stage II	38 (31.7)	30 (47.6)	8 (14.0)		12 (23.5)	6 (30.0)	6 (19.4)	
Stage III	61 (50.8)	20 (31.7)	41 (71.9)		31 (60.8)	10 (50.0)	21 (67.7)	
Stage IV	3 (2.5)	1 (1.6)	2 (3.5)		1 (2.0)	0 (0.0)	1 (3.2)	

*, P<0.05; ***, P<0.001. GC, gastric cancer; RRS, radiomics risk score; BMI, body mass index.

Table 2 Univariate and multivariate Cox analyses for OS of GC patients in the developing cohort.

Variables	Univariate Cox analysis				Multivariate Cox analysis			
	HR	HR.95L	HR.95H	P value	HR	HR.95L	HR.95H	P value
Age (>70 *vs.* ≤70)	1.11	0.61	2.03	0.741	–	–	–	–
Gender (male *vs.* female)	0.80	0.42	1.55	0.510	–	–	–	–
BMI (low *vs.* normal)	0.70	0.17	2.93	0.629	–	–	–	–
BMI (high *vs.* normal)	0.86	0.43	1.73	0.671	–	–	–	–
Anemia (yes *vs.* no)	1.42	0.80	2.51	0.233	–	–	–	–
Charlson score (≥2 *vs.* <2)	3.38	1.87	6.10	P<0.001***	2.38	1.18	4.82	0.016*
Location (body *vs.* cardia)	0.99	0.37	2.66	0.983	–	–	–	–
Location (pylorus *vs.* cardia)	1.30	0.56	2.99	0.539	–	–	–	–
Location (all *vs.* cardia)	2.24	0.71	7.08	0.168	–	–	–	–
Tumor size (≥3 *vs.* <3)	11.24	3.48	36.25	P<0.001***	4.47	1.24	16.07	0.022*
Nerve invasion (yes *vs.* no)	2.10	1.18	3.76	0.012*	1.16	0.58	2.32	0.670
Vascular invasion (yes *vs.* no)	1.51	0.82	2.79	0.187	–	–	–	–
Stage (stage II *vs.* stage I)	1.10	0.21	5.69	0.906	0.96	0.18	5.18	0.966
Stage (stage III *vs.* stage I)	7.50	1.80	31.17	0.006**	2.33	0.50	10.91	0.282
Stage (stage IV *vs.* stage I)	12.68	2.10	76.41	0.006**	1.98	0.27	14.53	0.502
RRS (high *vs.* low)	13.57	5.73	32.17	P<0.001***	6.94	2.79	17.28	<0.001***

*, P<0.05; **, P<0.01; ***, P<0.001. OS, overall survival; GC, gastric cancer; HR, hazard ratio; L, low; H, high; BMI, body mass index; RRS, radiomics risk score.

Table 3 Univariate and multivariate Cox analyses for DFS of GC patients in the developing cohort

Variables	Univariate Cox analysis				Multivariate Cox analysis			
	HR	HR.95L	HR.95H	P value	HR	HR.95L	HR.95H	P value
Age (>70 *vs.* ≤70)	0.93	0.56	1.56	0.786	–	–	–	–
Gender (male *vs.* Female)	0.93	0.53	1.63	0.802	–	–	–	–
BMI (low *vs.* Normal)	0.61	0.19	1.95	0.401	–	–	–	–
BMI (high *vs.* normal)	0.86	0.48	1.53	0.598	–	–	–	–
Anemia (yes *vs.* no)	1.13	0.70	1.82	0.613	–	–	–	–
Charlson score (≥2 *vs.* <2)	2.28	1.35	3.86	0.002**	1.34	0.70	2.56	0.379
Location (body *vs.* cardia)	1.22	0.54	2.80	0.631	1.60	0.69	3.75	0.275
Location (pylorus *vs.* cardia)	1.53	0.74	3.18	0.250	1.32	0.62	2.79	0.471
Location (all *vs.* cardia)	3.39	1.26	9.16	0.016*	2.15	0.61	7.59	0.235
Tumor size (≥3 *vs.* <3)	3.57	1.94	6.55	P<0.001***	2.47	1.19	5.14	0.016*
Nerve invasion (yes *vs.* no)	2.39	1.47	3.87	P<0.001***	2.02	1.08	3.80	0.029*
Vascular invasion (yes *vs.* no)	1.67	1.01	2.78	0.048*	1.31	0.67	2.57	0.434
Stage (stage II *vs.* stage I)	1.04	0.40	2.67	0.942	0.79	0.29	2.17	0.652
Stage (stage III *vs.* stage I)	2.68	1.14	6.32	0.024*	1.09	0.41	2.90	0.859
Stage (stage IV *vs.* stage I)	4.22	1.05	16.96	0.042*	0.53	0.07	3.71	0.521
RRS (high *vs.* low)	3.80	2.28	6.33	P<0.001***	2.71	1.47	5.02	0.001**

*, P<0.05; **, P<0.01; ***, P<0.001. DFS, disease-free survival; GC, gastric cancer; HR, hazard ratio; L, low; H, high; BMI, body mass index; RRS, radiomics risk score.

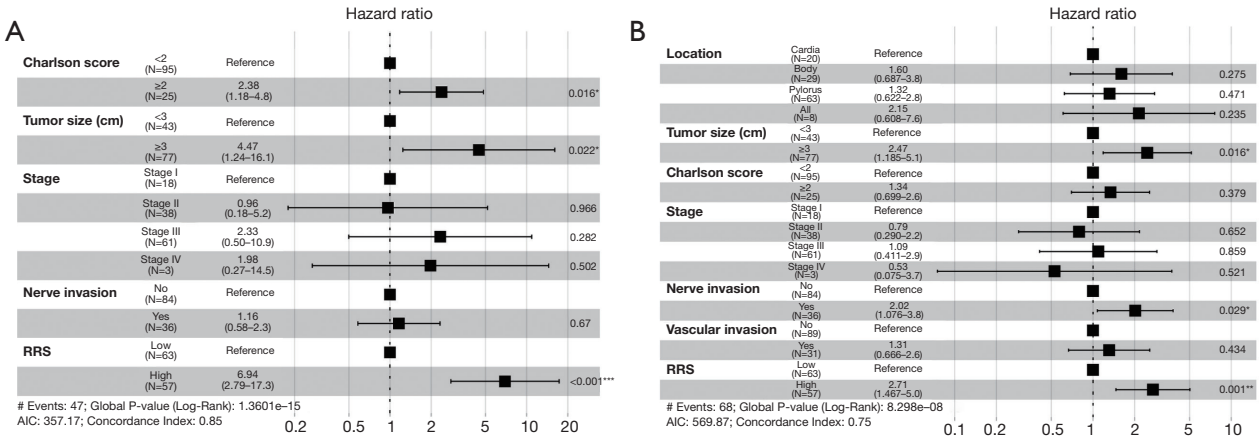

Figure 5 Multivariate Cox analysis of GC patients using the RRS combined with different clinicopathological characteristics in the developing cohort. (A) Multivariate Cox analysis for OS of RRS and different clinicopathological characteristics. (B) Multivariate Cox analysis for DFS of RRS and different clinicopathological characteristics. *, P<0.05; **, P<0.01; ***, P<0.001. GC, gastric cancer; RRS, radiomics risk score; AIC, Akaike information criterion; OS, overall survival; DFS, disease-free survival.

postoperative chemotherapy as needed, and 54 (52.43%) of them had a high-risk RRS. Among GC patients in the low-risk RRS group, Kaplan-Meier curve analysis showed that there was no significant difference in OS and DFS between patients who received postoperative chemotherapy and those who did not (OS: log-rank P=0.069, *Figure 4D*; DFS: log-rank P=0.497, *Figure 4E*). Interestingly, in the high-risk RRS group, the OS and DFS of patients who received postoperative chemotherapy were significantly improved compared with those who did not receive postoperative chemotherapy (OS: log-rank P<0.001, *Figure 4F*; DFS: log-rank P<0.001, *Figure 4G*). Therefore, GC patients with a higher RRS could benefit from postoperative chemotherapy, although there was no significant effect on patients with a lower RRS.

Development and validation of a radiomics nomogram to predict OS and DFS in GC patients

We performed univariate and multivariate Cox regression analyses of OS and DFS on RRS combined with different clinicopathological characteristics in the developing cohort (*Tables 2,3*). The results showed that a higher Charlson score (≥2), larger tumor size (≥3 cm), and higher RRS were independent risk factors for OS in GC patients from the developing cohort (P<0.05; *Figure 5A*). Furthermore, larger tumor size (≥3 cm), nerve invasion, and higher RRS were independent risk factors for DFS (P<0.05; *Figure 5B*). Therefore, based on the significant variables in the multivariate Cox regression analysis, we constructed nomograms for clinical prognosis prediction. The nomogram could predict the 1-, 2- and 3-year survival probability of GC patients according to the RRS and clinicopathological characteristics (OS: *Figure 6A*; DFS: *Figure 6B*). In the developing cohort, the C-index was 0.835 [95% confidence interval (CI): 0.793–0.877] for OS and 0.733 (95% CI: 0.677–0.789) for DFS. The discrimination performance was also analyzed in the validation cohort, and the results showed that the nomogram had better predictive ability [OS: 0.730 (95% CI: 0.638–0.822); DFS: 0.695 (95% CI: 0.602–0.788)]. The 1-, 2-, and 3-year nomogram calibration curves displayed better agreement between the estimated and actual observations in the developing and validation cohorts (*Figure 6C-6F*). Moreover, DCA showed that using the nomogram model to predict the prognosis of GC patients would be more beneficial than the all-treatment or no-treatment method or than using the clinicopathological characteristics model alone (OS: *Figure 7A*; DFS: *Figure 7B*). It can be seen that the net benefit of using the nomogram was higher. Moreover, we calculated the corresponding RQS points for this study to evaluate the quality of the radiomics research. The results indicated a total RQS score of 18.0. The detailed scoring criteria are presented in Table S2.

Discussion

Although the development of better diagnostic and

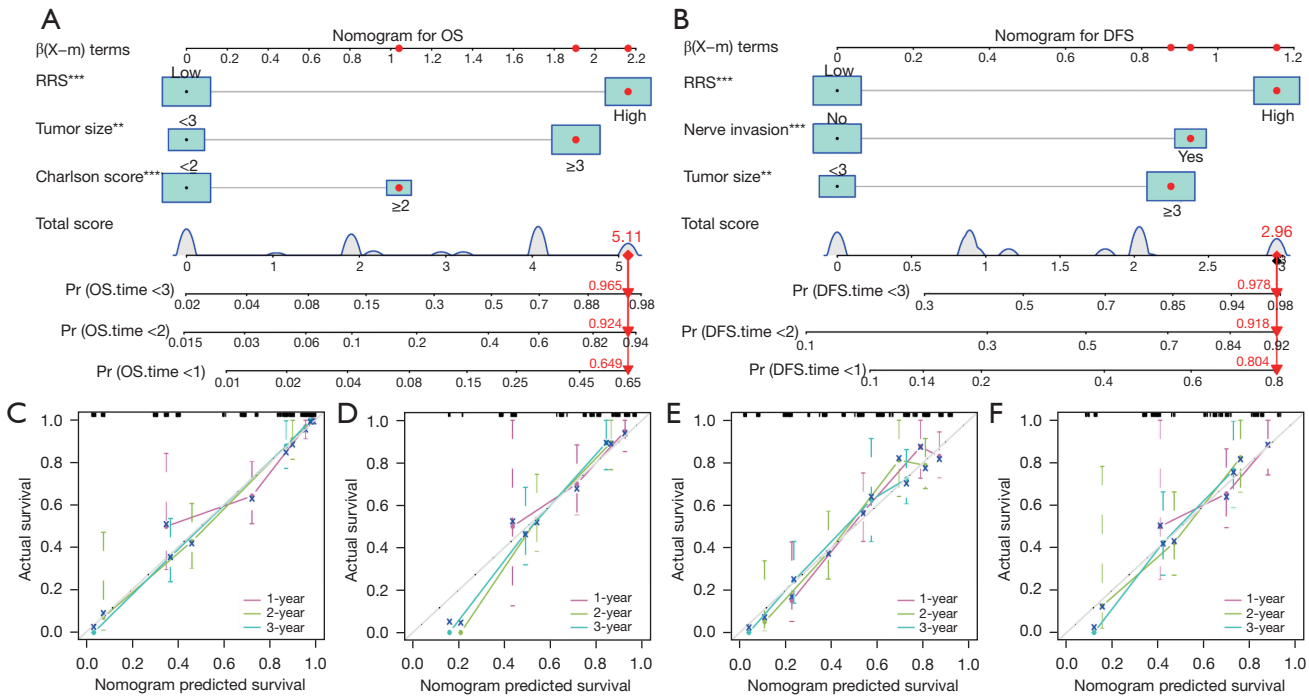

Figure 6 Construction and validation of the nomogram to predict the survival of GC patients. (A) A nomogram was constructed to predict the OS of GC patients using the RRS and different clinicopathological characteristics from multivariate Cox analysis. (B) A nomogram was constructed to predict the DFS of GC patients using the RRS and different clinicopathological characteristics. (C,D) The predictive effect of the nomogram on the OS of GC patients was validated using the calibration curve in the developing (C) and validation (D) cohorts. (E,F) The predictive effect of the nomogram on the DFS of GC patients was validated using the calibration curve in the developing (E) and validation (F) cohorts. **, P<0.01; ***, P<0.001. GC, gastric cancer; OS, overall survival; RRS, radiomics risk score; DFS, disease-free survival.

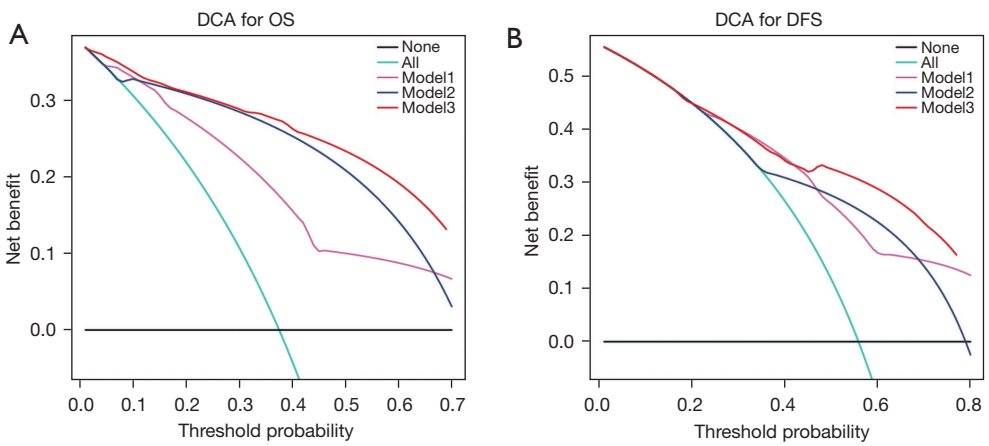

Figure 7 DCA was performed to display the benefit for predicting the survival of GC patients. (A,B) DCA of the nomogram to predict OS (A) and DFS (B). The abscissa represents the threshold probability, and the ordinate represents the net benefit of the patient. The black line indicates the benefit of patients without treatment, and the blue line indicates the benefits of all patients receiving treatment. The pink line, dark blue line and red line represent the benefit ratio of GC patients under three different models. Model 1 used only the clinicopathological characteristics in the nomogram, Model 2 used the RRS, and Model 3 used the nomogram to evaluate the survival of patients. DCA, decision curve analysis; GC, gastric cancer; OS, overall survival; DFS, disease-free survival.

treatment approaches have significantly contributed to reducing GC incidence and mortality rates in recent years, this tumor type is still very important in many areas of the world. Therefore, it is essential to develop an accurate prognosis prediction model to ensure the hierarchical analysis of prognosis and acceptance of personalized treatment programs for GC patients. This study was the first attempt to combine radiomics features with 8 machine learning algorithms and 29 algorithm combinations to build an optimal model for the prognosis of GC tumor tissue. The RRS model successfully predicted the OS and DFS of GC patients. Moreover, GC patients with a higher RRS benefited from postoperative chemotherapy, which further proves this to be an excellent prediction model. By combining clinicopathological characteristics and the RRS risk model, we also constructed a nomogram to provide personalized and accurate treatment for GC patients.

Radiomics is an emerging tool that can quantitatively identify tissue characteristics from medical images and predict the prognosis of cancer patients. Shin *et al.* used a radiomics model to predict the relapse-free survival (RFS) of patients with advanced GC (32). In the training cohort, the C-index of the prediction model for RFS was 0.719 (95% CI: 0.674–0.764). Li *et al.* built a radiomics signature based on intratumoral and peritumoral regions to predict the DFS of patients (33). The results showed that the radiomics signature was an independent risk factor for the prognosis of patients. Moreover, Zhang *et al.* further built a radiomics prediction model for early recurrence in patients with advanced GC (34). However, these models only used single or traditional machine learning algorithms to search for key radiomics features, which may miss some important features. In this study, on the basis of LASSO Cox analysis and the GBM model, we screened 11 radiomics features that were significantly correlated with prognosis. Then, we further constructed and validated a stable and effective RRS to predict the prognosis and postoperative chemotherapy benefits of GC patients. The RRS had a better predictive ability for the OS and DFS of GC patients in the developing and validation cohorts. Therefore, the RRS could accurately provide useful information to distinguish the different survival risks of GC patients. This helps us to identify subgroups of patients with poor prognosis and provide more intensive treatment and closer follow-up plans.

Current guidelines recommend adjuvant chemotherapy as a standard component for advanced GC therapies (35). However, many studies have reported that a proportion of patients do not benefit from current chemotherapy strategies (36,37). The optimal criteria for the selection of candidates remain controversial. Thus, the accurate identification of subgroups of patients will improve the prognostic system and lead to more personalized therapy. In our study, the RRS was capable of stratifying patients into groups with different sensitivities to chemotherapy. The results further demonstrated that chemotherapy results in a significantly better clinical outcome in GC patients with a high RRS, whereas those patients with a low RRS did not obtain benefits from postoperative chemotherapy. This could help us identify the subgroup of patients who would benefit less from chemotherapy and for whom alternative treatment strategies could be tested, such as using less toxic and more tolerable systemic therapy or close surveillance, or first-line immune checkpoint inhibitors. Therefore, our CT image-based RRS for patients with GC was a powerful and effective tool to predict prognosis and benefits from postoperative chemotherapy. In other words, patients with a higher RRS have a higher likelihood of recurrence and death but experience a clear benefit from chemotherapy. This may be related to intratumoral heterogeneity, as well as the different expression of biological phenotypes such as cell death and the cell cycle pathway in radiation characteristics. The potential mechanisms need to be further explored in follow-up multi-omics research on radiomics, genomics, transcriptomics, microbiome, and proteomics.

There are recognized limitations to this study. First, according to the inclusion and exclusion criteria, we screened 504 GC patients from January 2014 to December 2016, and 172 GC patients were finally enrolled in the follow-up study and analysis. Moreover, the sample number in this study was relatively small and from a single cohort. We need to further increase the sample size in subsequent studies to verify the consistency of the model. Second, all GC patients included in the study underwent radical surgery. Therefore, the number of patients with advanced GC in stage IV or who could not be treated surgically due to distant metastasis was relatively small. This may result in a certain deviation in the accuracy of clinical application. Finally, this study focused on the radiomics features of tumor tissue to predict the clinical outcome of GC patients. However, the similarities and differences between normal tissues, surrounding tissues and tumor tissues also need further study.

Conclusions

In conclusion, this study resulted in the construction of a

stable prognosis prediction model for GC patients based on the combination of multiple machine learning algorithms. As a novel biomarker, the RRS could effectively and accurately predict the clinical outcome, disease recurrence, and the benefits of postoperative chemotherapy. The RRS combined with clinicopathological features could further promote the practicability of the clinical prediction model and provide help for personalized treatment of GC patients.

Acknowledgments

We thank the International Science & Technology Cooperation Base for Tumor Transformation Research of Zhejiang Province and the International Science & Technology Cooperation Base for Research on Interaction between Tumor-related Pathogens and Hosts of Zhejiang Province for consultation and instrument availability that supported this work.

Funding: This study was supported by grants from the Zhejiang Provincial Health Department Medical Support Discipline-Nutrition (Grant No. 11-ZC24 to Qiantong Dong), the Special Fund of Zhejiang Upper Gastrointestinal Tumor Diagnosis and Treatment Technology Research Center (Grant No. jbzx-202006 to Qiantong Dong), the Fund of the Society of Parenteral and Enteral Nutrition of Chinese Medical Association (Grant No. Z-2017-24-2211 to Qiantong Dong), the National Key Clinical Specialty (General Surgery), the First Affiliated Hospital of Wenzhou Medical University (to Qiantong Dong), the Natural Science Foundation of Zhejiang Province (Grant No. LY20H160015 to Mingdong Lu), and the Project of Zhejiang Provincial Department of Education (Grant No. Y202147047 to Mingdong Lu).

Footnote

Reporting Checklist: The authors have completed the CLEAR and TRIPOD reporting checklists. Available at https://jgo.amegroups.com/article/view/10.21037/jgo-23-627/rc

Data Sharing Statement: Available at https://jgo.amegroups.com/article/view/10.21037/jgo-23-627/dss

Peer Review File: Available at https://jgo.amegroups.com/article/view/10.21037/jgo-23-627/prf

Conflicts of Interest: All authors have completed the ICMJE uniform disclosure form (available at https://jgo.amegroups.com/article/view/10.21037/jgo-23-627/coif). ML reports funding support from the Natural Science Foundation of Zhejiang Province (Grant No. LY20H160015) and the Project of Zhejiang Provincial Department of Education (Grant No. Y202147047). EDN received financial support from Conselho Nacional de Desenvolvimento Científico e Tecnológico (CNPq) and Fundação de Amparo à Pesquisa do Estado de São Paulo (FAPESP – 2014/26897-0). QD reports funding from the Zhejiang Provincial Health Department Medical Support Discipline-Nutrition (Grant No. 11-ZC24), the Special Fund of Zhejiang Upper Gastrointestinal Tumor Diagnosis and Treatment Technology Research Center (Grant No. jbzx-202006), the Fund of the Society of Parenteral and Enteral Nutrition of Chinese Medical Association (Grant No. Z-2017-24-2211), the National Key Clinical Specialty (General Surgery), the First Affiliated Hospital of Wenzhou Medical University. The other authors have no conflicts of interest to declare.

Ethical Statement: The authors are accountable for all aspects of the work in ensuring that questions related to the accuracy or integrity of any part of the work are appropriately investigated and resolved. The study was conducted in accordance with the Declaration of Helsinki (as revised in 2013). The study was approved by the Ethics Committee of the First Affiliated Hospital of Wenzhou Medical University (No. KY2021-R092). Considering this was a retrospective study that did not impose additional costs or harm on patients, informed consent from the patients was not required.

References

1. Siegel RL, Miller KD, Wagle NS, et al. Cancer statistics, 2023. CA Cancer J Clin 2023;73:17-48.
2. Chen W, Zheng R, Zeng H, et al. Annual report on status of cancer in China, 2011. Chin J Cancer Res 2015;27:2-12.
3. Pavlakis N, Sjoquist KM, Martin AJ, et al. Regorafenib

for the Treatment of Advanced Gastric Cancer (INTEGRATE): A Multinational Placebo-Controlled Phase II Trial. J Clin Oncol 2016;34:2728-35.
4. Bando E, Makuuchi R, Tokunaga M, et al. Impact of clinical tumor-node-metastasis staging on survival in gastric carcinoma patients receiving surgery. Gastric Cancer 2017;20:448-56.
5. Chen D, Fu M, Chi L, et al. Prognostic and predictive value of a pathomics signature in gastric cancer. Nat Commun 2022;13:6903.
6. Li J, Yin H, Wang Y, et al. Multiparametric MRI-based radiomics nomogram for early prediction of pathological response to neoadjuvant chemotherapy in locally advanced gastric cancer. Eur Radiol 2023;33:2746-56.
7. Jiang Y, Chen C, Xie J, et al. Radiomics signature of computed tomography imaging for prediction of survival and chemotherapeutic benefits in gastric cancer. EBioMedicine 2018;36:171-82.
8. Gillies RJ, Kinahan PE, Hricak H. Radiomics: Images Are More than Pictures, They Are Data. Radiology 2016;278:563-77.
9. Lambin P, Rios-Velazquez E, Leijenaar R, et al. Radiomics: extracting more information from medical images using advanced feature analysis. Eur J Cancer 2012;48:441-6.
10. Ma Z, Fang M, Huang Y, et al. CT-based radiomics signature for differentiating Borrmann type IV gastric cancer from primary gastric lymphoma. Eur J Radiol 2017;91:142-7.
11. Ma T, Cui J, Wang L, et al. A CT-based radiomics signature for prediction of HER2 overexpression and treatment efficacy of trastuzumab in advanced gastric cancer. Transl Cancer Res 2022;11:4326-37.
12. Yang J, Wu Q, Xu L, et al. Integrating tumor and nodal radiomics to predict lymph node metastasis in gastric cancer. Radiother Oncol 2020;150:89-96.
13. Wang T, She Y, Yang Y, et al. Radiomics for Survival Risk Stratification of Clinical and Pathologic Stage IA Pure-Solid Non-Small Cell Lung Cancer. Radiology 2022;302:425-34.
14. Yu Y, Tan Y, Xie C, et al. Development and Validation of a Preoperative Magnetic Resonance Imaging Radiomics-Based Signature to Predict Axillary Lymph Node Metastasis and Disease-Free Survival in Patients With Early-Stage Breast Cancer. JAMA Netw Open 2020;3:e2028086.
15. Wang X, Xie T, Luo J, et al. Radiomics predicts the prognosis of patients with locally advanced breast cancer by reflecting the heterogeneity of tumor cells and the tumor microenvironment. Breast Cancer Res 2022;24:20.
16. Dong Z, Liu G, Tu L, et al. Establishment of a prediction model of postoperative infection complications in patients with gastric cancer and its impact on prognosis. J Gastrointest Oncol 2023;14:1250-8.
17. Hu Y, Xie C, Yang H, et al. Assessment of Intratumoral and Peritumoral Computed Tomography Radiomics for Predicting Pathological Complete Response to Neoadjuvant Chemoradiation in Patients With Esophageal Squamous Cell Carcinoma. JAMA Netw Open 2020;3:e2015927.
18. Mao N, Shi Y, Lian C, et al. Intratumoral and peritumoral radiomics for preoperative prediction of neoadjuvant chemotherapy effect in breast cancer based on contrast-enhanced spectral mammography. Eur Radiol 2022;32:3207-19.
19. Avanzo M, Wei L, Stancanello J, et al. Machine and deep learning methods for radiomics. Med Phys 2020;47:e185-202.
20. Mao B, Ma J, Duan S, et al. Preoperative classification of primary and metastatic liver cancer via machine learning-based ultrasound radiomics. Eur Radiol 2021;31:4576-86.
21. Li Z, Chen L, Song Y, et al. Predictive value of magnetic resonance imaging radiomics-based machine learning for disease progression in patients with high-grade glioma. Quant Imaging Med Surg 2023;13:224-36.
22. Japanese gastric cancer treatment guidelines 2010 (ver. 3). Gastric Cancer 2011;14:113-23.
23. Wang FH, Shen L, Li J, et al. The Chinese Society of Clinical Oncology (CSCO): clinical guidelines for the diagnosis and treatment of gastric cancer. Cancer Commun (Lond) 2019;39:10.
24. Ajani JA, Bentrem DJ, Besh S, et al. Gastric cancer, version 2.2013: featured updates to the NCCN Guidelines. J Natl Compr Canc Netw 2013;11:531-46.
25. Ajani JA, D'Amico TA, Almhanna K, et al. Gastric Cancer, Version 3.2016, NCCN Clinical Practice Guidelines in Oncology. J Natl Compr Canc Netw 2016;14:1286-312.
26. Kocak B, Baessler B, Bakas S, et al. CheckList for EvaluAtion of Radiomics research (CLEAR): a step-by-step reporting guideline for authors and reviewers endorsed by ESR and EuSoMII. Insights Imaging 2023;14:75.
27. Zwanenburg A, Vallières M, Abdalah MA, et al. The Image Biomarker Standardization Initiative: Standardized Quantitative Radiomics for High-Throughput Image-based Phenotyping. Radiology 2020;295:328-38.
28. van Griethuysen JJM, Fedorov A, Parmar C, et al.

Computational Radiomics System to Decode the Radiographic Phenotype. Cancer Res 2017;77:e104-7.
29. Pan B, Zhang W, Chen W, et al. Establishment of the Radiologic Tumor Invasion Index Based on Radiomics Splenic Features and Clinical Factors to Predict Serous Invasion of Gastric Cancer. Front Oncol 2021;11:682456.
30. Liu Z, Liu L, Weng S, et al. Machine learning-based integration develops an immune-derived lncRNA signature for improving outcomes in colorectal cancer. Nat Commun 2022;13:816.
31. Lambin P, Leijenaar RTH, Deist TM, et al. Radiomics: the bridge between medical imaging and personalized medicine. Nat Rev Clin Oncol 2017;14:749-62.
32. Shin J, Lim JS, Huh YM, et al. A radiomics-based model for predicting prognosis of locally advanced gastric cancer in the preoperative setting. Sci Rep 2021;11:1879.
33. Li J, Zhang C, Wei J, et al. Intratumoral and Peritumoral Radiomics of Contrast-Enhanced CT for Prediction of Disease-Free Survival and Chemotherapy Response in Stage II/III Gastric Cancer. Front Oncol 2020;10:552270.
34. Zhang W, Fang M, Dong D, et al. Development and validation of a CT-based radiomic nomogram for preoperative prediction of early recurrence in advanced gastric cancer. Radiother Oncol 2020;145:13-20.
35. Noh SH, Park SR, Yang HK, et al. Adjuvant capecitabine plus oxaliplatin for gastric cancer after D2 gastrectomy (CLASSIC): 5-year follow-up of an open-label, randomised phase 3 trial. Lancet Oncol 2014;15:1389-96.
36. Jiang Y, Li T, Liang X, et al. Association of Adjuvant Chemotherapy With Survival in Patients With Stage II or III Gastric Cancer. JAMA Surg 2017;152:e171087.
37. Cheong JH, Yang HK, Kim H, et al. Predictive test for chemotherapy response in resectable gastric cancer: a multi-cohort, retrospective analysis. Lancet Oncol 2018;19:629-38.

Cite this article as: Xiang Y, Hu Y, Chen C, Zhi H, Zhang Z, Lu M, Chen X, Luo Z, Chen S, Dias-Neto E, Pizzini P, Chen X, Chen X, Zhuang Y, Dong Q. Radiomics based on machine learning algorithms could predict prognosis and postoperative chemotherapy benefits of patients with gastric cancer: a retrospective cohort study. J Gastrointest Oncol 2023;14(5):2048-2063. doi: 10.21037/jgo-23-627

Supplementary

Table S1 Clinicopathological characteristics of the patients in the developing and validation cohorts

Variables	All patients (n=171)	GC patients		P value
		Developing cohort (n=120)	Validation cohort (n=51)	
Age (years)				0.362
≤70	111 (64.9)	81 (67.5)	30 (58.8)	
>70	60 (35.1)	39 (32.5)	21 (41.2)	
Gender				0.822
Female	40 (23.4)	27 (22.5)	13 (25.5)	
Male	131 (76.6)	93 (77.5)	38 (74.5)	
BMI				0.829
Low	9 (5.3)	7 (5.8)	2 (3.9)	
Normal	125 (73.1)	86 (71.7)	39 (76.5)	
High	37 (21.6)	27 (22.5)	10 (19.6)	
Anemia				0.223
No	91 (53.2)	68 (56.7)	23 (45.1)	
Yes	80 (46.8)	52 (43.3)	28 (54.9)	
Charlson score				0.022*
<2	143 (83.6)	95 (79.2)	48 (94.1)	
≥2	28 (16.4)	25 (20.8)	3 (5.9)	
Location				0.340
Cardia	33 (19.3)	20 (16.7)	13 (25.5)	
Body	38 (22.2)	29 (24.2)	9 (17.6)	
Pylorus	91 (53.2)	63 (52.5)	28 (54.9)	
All	9 (5.3)	8 (6.7)	1 (2.0)	
Tumor size (cm)				0.700
<3	59 (34.5)	43 (35.8)	16 (31.4)	
≥3	112 (65.5)	77 (64.2)	35 (68.6)	
Nerve invasion				0.680
No	122 (71.3)	84 (70.0)	38 (74.5)	
Yes	49 (28.7)	36 (30.0)	13 (25.5)	
Vascular invasion				0.499
No	130 (76.0)	89 (74.2)	41 (80.4)	
Yes	41 (24.0)	31 (25.8)	10 (19.6)	
Stage				0.685
Stage I	25 (14.6)	18 (15.0)	7 (13.7)	
Stage II	50 (29.2)	38 (31.7)	12 (23.5)	
Stage III	92 (53.8)	61 (50.8)	31 (60.8)	
Stage IV	4 (2.3)	3 (2.5)	1 (2.0)	

*, P<0.05.

https://dx.doi.org/10.21037/jgo-23-627

Table S2 The result of radiomics quality score in this study

ID	Research details	Research purpose	RQS point
1	Image protocol quality	To ensure the repeatability of the experiment	1.0
2	Multiple segmentation	To analyze the impact of different segmentation methods on features	1.0
3	Phantom study	To analyze the impact of different machine types on features	0.0
4	Imaging at multiple time points	To analyze the impact of temporal heterogeneity, such as organ motion	0.0
5	Feature reduction or adjustment for multiple testing	To prevent overfitting	3.0
6	Multivariable analysis	To increase the clinical practicality of radiomics	1.0
7	Biological correlates	To find the connection between radiomics and biological mechanisms	0.0
8	Cut-off analysis	To reduce the risk of optimistic estimation	1.0
9	Discrimination statistics	To reflect the predictive performance of the model	2.0
10	Prospective study	To provide the highest level of evidence for radiomics research	0.0
11	Calibration statistics	To reflect the stability of the model	2.0
12	Validation	To increase the credibility of the model	2.0
13	Comparison to gold standard	To demonstrate the additional value of radiomics	0.0
14	Cost-effectiveness analysis	To report on the clinical significance of radiomics	2.0
15	Cost-effectiveness analysis	To increase the clinical significance of radiomics	0.0
16	Open science and data	To promote knowledge transformation and improve the repeatability of radiomics	3.0
Total points			18.0

https://dx.doi.org/10.21037/jgo-23-627